

Rattling mode and symmetry lowering resulting from instability of B₁₂-molecule in LuB₁₂

N.Sluchanko,^{1,2,*} A.Bogach,¹ N.Bolotina,³ V.Glushkov,^{1,2} S.Demishev,^{1,4} A.Dudka,³
V.Krasnorussky,¹ O.Khrykina,³ K.Krasikov,⁴ V.Mironov,³ V.Filipov,⁵ and N.Shitsevalova⁵

¹*Prokhorov General Physics Institute, Russian Academy of Sciences, 38 Vavilov Str., 119991 Moscow, Russia*

²*National University of Science and Technology (MISiS), 119049 Moscow, Russia*

³*Shubnikov Institute of Crystallography of Federal Scientific Research Centre Crystallography and Photonics of Russian Academy of Sciences, 59 Leninskii Ave., 119333 Moscow, Russia*

⁴*Moscow Institute of Physics and Technology (State University), 9 Institutskiy Per., 141700 Dolgoprudny, Russia*

⁵*Frantsevich Institute for Problems of Materials Science, National Academy of Sciences of Ukraine, 3 Krzhyzhanovsky Str., 03680 Kiev, Ukraine*

(Dated: July 10, 2017)

The dodecaboride LuB₁₂ with cage-glass state and rattling modes has been studied to clarify the nature of the large amplitude vibrations of Lu ions. Discovered anisotropy of charge transport in conjunction with distortions of the conventional *fcc* symmetry of the crystal lattice may be attributed to coherent motion of Lu ions along singular direction in the lattice. Arguments are presented in favor of cooperative dynamic Jahn-Teller effect in the boron sublattice to be the reason of the rattling mode, lattice distortion and formation of the filamentary structure of the conductive channels.

PACS numbers: 61.66.Fn, 72.15.Gd:

Introduction. – Rattling compounds have attracted wide interest in the last few decades due to their intriguing and exotic physical properties. Rattling effect (a large amplitude vibration of an atom in an oversized atomic cage) can be responsible for an extremely low thermal conductivity and high thermoelectric efficiency in various cage compounds, such as filled skutterudites [1], β -pyrochlore oxides [2], clathrates [3], RT_2Zn_{20} ($R = \text{Pr, La; T} = \text{Ir, Ru}$) [4], quadruple perovskites [5], higher borides RB_{12} [6], etc. These local excitations may also affect the electronic properties of solids due to strong electron-phonon coupling [6]. The nature of rattling motion and the mechanisms of its influence on the unusual properties and exotic ground states is still under question.

Among rattling compounds the rare earth and transition metal dodecaborides RB_{12} ($R = \text{Y, Zr, Tb-Lu}$) represent the simplest, model objects with face-centered cubic (*fcc*) NaCl-type crystal lattice (space group $Fm\bar{3}m-O5h$) built by B₁₂ cubooctahedra and metal atoms R centered in the large cubooctahedral cages B₂₄ formed by six neighboring B₁₂ units (Fig. 1a,b). Strong covalent bonds between boron atoms (both within B₁₂ units and between them) form a rigid boron framework (Fig. 1b), which changes insignificantly in the RB_{12} family. Large difference between the size of B₂₄ cage ($r(\text{B}_{24}) \sim 1.1 - 1.15\text{\AA}$ [7]), and the radius of metallic ions ($0.8 - 0.97\text{\AA}$) leads to a formation of loosely bound state of the heavy ion in the rigid B₂₄ cage, resulting in low frequency (14 – 18 meV [8]) dispersion-less (Einstein-like, rattling) vibrations in the phonon spectrum of dodecaborides. The electron deficiency in the boron lattice is compensated by transfer of two valence electrons ($6s^2$) from each R atom to B₁₂ cluster, while the third valence electron ($5d^1$) in RB_{12}

enters the conduction band. So, all rare earth dodecaborides are good metals, in which conduction band at the Fermi level is mainly contributed from $5d$ -states with a small admixture of B $2p$ -electrons [9]. The only exception is a narrow-gap semiconductor YbB₁₂ with exotic insulating ground state, which is observed in the regime of strong charge and spin fluctuations. Besides, YbB₁₂ undergoes a metal-insulator transition at $T^* \sim 60$ K [6, 7, 10]. Thus, these RB_{12} rattling compounds cover a variety of ground states and the regimes of charge transport, that ranges from the unusual superconductivity in LuB₁₂ and ZrB₁₂ [7] and Kondo insulator [6, 7, 10] or topological crystalline insulator behaviour [11] predicted for YbB₁₂ to the complicated magnetic ordering and peculiar incommensurate magnetic structures detected for TbB₁₂-TmB₁₂ antiferromagnets [7].

It is particularly important that there are some experimental evidences for the local structural distortions in the cubic lattice of RB_{12} at low temperatures. It has been recently concluded [12] that these dodecaborides RB_{12} tend to form a cage-glass phase through the order-disorder phase transition (at $T^* \sim 60$ K in LuB₁₂), that results in freezing of R ions in the random positions inside the B₂₄ cages. Besides, x-ray diffraction studies [13] discovered a significant tetragonal distortion of the atomic structure of LuB₁₂ in the vicinity of this phase transition.

Given that LuB₁₂ is a reference compound for the family of RB_{12} , it is important (*i*) to investigate an interplay between the rattling effect and features of crystalline and electronic structure and (*ii*) to shed more light on the nature of rattling in this non-magnetic dodecaboride. Analysing the influence of rattling mode on the transport and structural properties of LuB₁₂ we studied in detail the changes of crystal structure and the anisotropy of

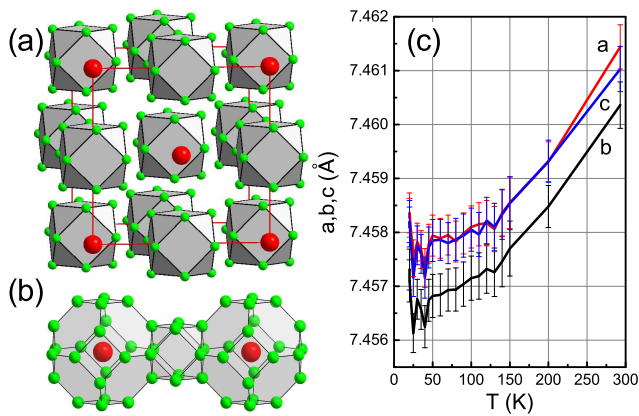


FIG. 1. (Color online) (a) a NaCl-like unit cell of LuB₁₂, with Lu (red spheres) as Na and B₁₂ clusters (green spheres) as Cl. (b) two large B₂₄ polyhedra centred by Lu atoms and a smaller B₁₂ cubooctahedron between them. (c) The temperature dependence of the lattice parameters a , b and c .

charge carriers scattering developed at low temperatures in the cage-glass state of LuB₁₂. Then, searching for the mechanism governing the large amplitude vibration of R ion we present here the results of quantum chemical calculations and geometry optimizations for negatively charged [B₁₂]²⁻ cluster. Our results argue in favour of a cooperative dynamic Jahn-Teller effect in the boron sublattice as a possible mechanism responsible for the rattling modes, structural distortions and charge transport anisotropy in LuB₁₂.

Experimental results. – Details of experiment are given in Supplementary materials [14]. Precise x-ray diffraction reflexes and quantum oscillations of magnetization (see Figs. in [14]), testify to the high quality of the crystals. The [100]- and [010]- elongated rectangular samples (#1 and #2 hereafter) with equally oriented (100), (010) and (001) faces were cut from one ingot of LuB₁₂ (Fig.2c). The resistivity $\rho(T)$ curves for LuB₁₂ crystals #1 (measuring current $\mathbf{I}||[100]$) and #2 ($\mathbf{I}||[010]$), are shown (Fig.2a) in the absence of an external magnetic field ($H = 0$, curves 1 and 2 correspondingly) and in steady magnetic field of 80 kOe directed along the crystal axes $[00\bar{1}]$ (curve 3 for #1, curve 4 for #2), $[0\bar{1}0]$ (curve 5 for #1) and $[\bar{1}00]$ (curve 6 for #1 and 7 for #2). A significant anisotropy of the transverse magnetoresistance ($\sim 20\%$) is observed below $T^* \sim 60$ K at $H = 80$ kOe, especially for the crystal #2 (see curves 4 and 6 in Fig.2a, 2b for comparison), in spite of the fact that \mathbf{H} -directions $[00\bar{1}]$ and $[\bar{1}00]$ are symmetry-equivalent in cubic crystals. In addition, a minimum is observed below T^* on the dependences $\rho(T, H = 80 \text{ kOe})$ and the temperature lowering is accompanied with a growth of resistivity (see Fig.2b). Such behaviour cannot be attributed to the Kondo scattering of charge carriers, because it is accompanied with a large positive magnetoresistance in these LuB₁₂ crystals. Note that the resistiv-

ity $\rho(T, H = 80 \text{ kOe})$ minimum below T^* is accompanied with a maximum in the vicinity of 60 K on the $R_H(T)$ curves for $\mathbf{I}||[110]$, which was detected earlier both in Lu^{*N*}B₁₂ with various isotopic composition in boron (N -natural, 10 and 11) [15] and in substitutional solid solutions Zr_{1-x}Lu_xB₁₂ [16] and this anomaly of Hall effect was associated with the transition to the cage-glass state.

To clarify the nature of the anisotropy of the transverse magnetoresistance at low temperatures, angular dependences $\rho(\varphi)$ were measured at 2-4.2 K in the magnetic fields up to 80 kOe by rotating the crystals #1 and #2 around their current axes. Families of curves $\rho_1(\varphi)$ for $\mathbf{I}||[100]$ (sample #1) and $\rho_2(\varphi)$ for $\mathbf{I}||[010]$ (sample #2) are shown in Fig.2d. Evidently, the angular dependences of $\rho_2(\varphi)$ do not correspond to those expected for a cubic structure. As mentioned above, the great difference is recorded for $\mathbf{H}||[00\bar{1}]$ ($\varphi = 0^\circ$) and $\mathbf{H}||[\bar{1}00]$ ($\varphi = 90^\circ$), although these directions are equivalent in cubic crystals. On the contrary, the sample #1 gives a set of $\rho_1(\varphi)$ singularities corresponding to practically equivalent directions $[00\bar{1}]$, $[0\bar{1}0]$ (see Fig.2d and [14]). The anisotropy of magnetoresistance is clearly resolved in the polar coordinates in Fig.2e, where the difference $\rho_2(\varphi) - \rho_1(\varphi) = f(\varphi, H)$ is presented in the coloured picture. It is clearly discerned from Fig.2e that conduction channels, which are transverse to the plane (001), appear in the LuB₁₂ matrix.

Crystal structure. – In accordance with arguments presented in [13], the *fcc* symmetry of LuB₁₂ is notably distorted at low temperatures. Conventional software for the structure analysis results in calculated electron density (ED) replicating the symmetry of structure model if even the symmetry of real ED is distorted. To provide the ability to derive probable violations of symmetry from difference Fourier maps, the crystal structure must be analysed using a less symmetrical model (see [14] for details). Unit-cell values of LuB₁₂ were refined without any symmetry restriction over the temperature range 20-300 K. Very small (~ 0.001 Å, see Fig.1c) but steady difference of the lattice constants a, b, c was revealed, which was not accompanied by steady deviation of angular parameters from 90° . Cubic metric of the unit cell was kept, since revealed differences in the unit-cell values $b \neq a \cong c$ (Fig.1c) was too small to influence on a result of the structure refinement. Thermal vibration of the Lu ions was described by an isotropic parameter in order that assumed anisotropy of residual ED near the Lu site could reveal itself most clearly.

Difference Fourier maps were built based on the results of the $Fm\bar{3}m$ structure refinement at temperatures 90 and 295 K (Fig. 3, see [14] for details). Each Lu site in the cubic $Fm\bar{3}m$ structure lies at the intersection of three 4-fold axes perpendicular to three faces of the cubic cell. As may be seen (Fig.3a,b), residual ED distribution near Lu($0, \frac{1}{2}, \frac{1}{2}$) in the $x = 0$ face is not bound by a 4-fold axis even at room temperature, what does not actually agree with $Fm\bar{3}m$.

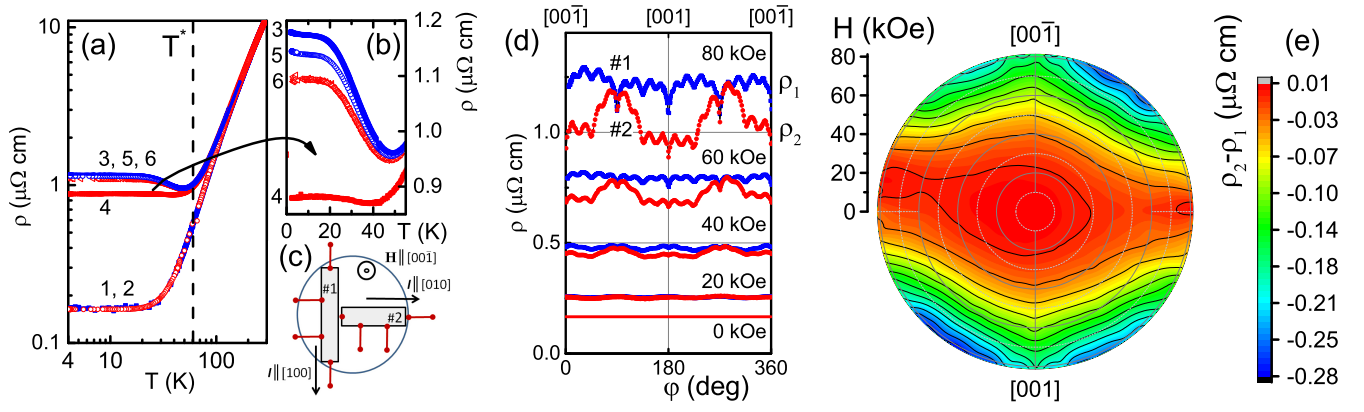


FIG. 2. (Color online) (a,b) Temperature dependences of the resistivity $\rho(T)$ for LuB_{12} crystals #1 ($\mathbf{I} \parallel [100]$) and #2 ($\mathbf{I} \parallel [010]$) are shown in the absence of an external magnetic field ($H = 0$, curves 1,2 correspondingly) and in steady magnetic field of 80 kOe directed along the crystal axes $[00\bar{1}]$ (curve 3 for #1, curve 4 for #2), $[0\bar{1}0]$ (curve 5 for #1) and $[\bar{1}00]$ (curve 6 for #2). (c) Two $[100]$ and $[010]$ -elongated rectangular samples #1 and #2 with equally oriented (100) , (010) and (001) faces were cut out from one single-crystalline disk of LuB_{12} . Angular dependences of $\rho_1(\varphi)$ and $\rho_2(\varphi)$ obtained rotating correspondingly the crystals #1 and #2 around their current axes in various magnetic fields up to 80 kOe at temperatures 2 - 4.2K. (e) The anisotropy of magnetoresistance $\rho_2(\varphi) - \rho_1(\varphi) = f(\varphi, H)$ presented in the polar coordinates.

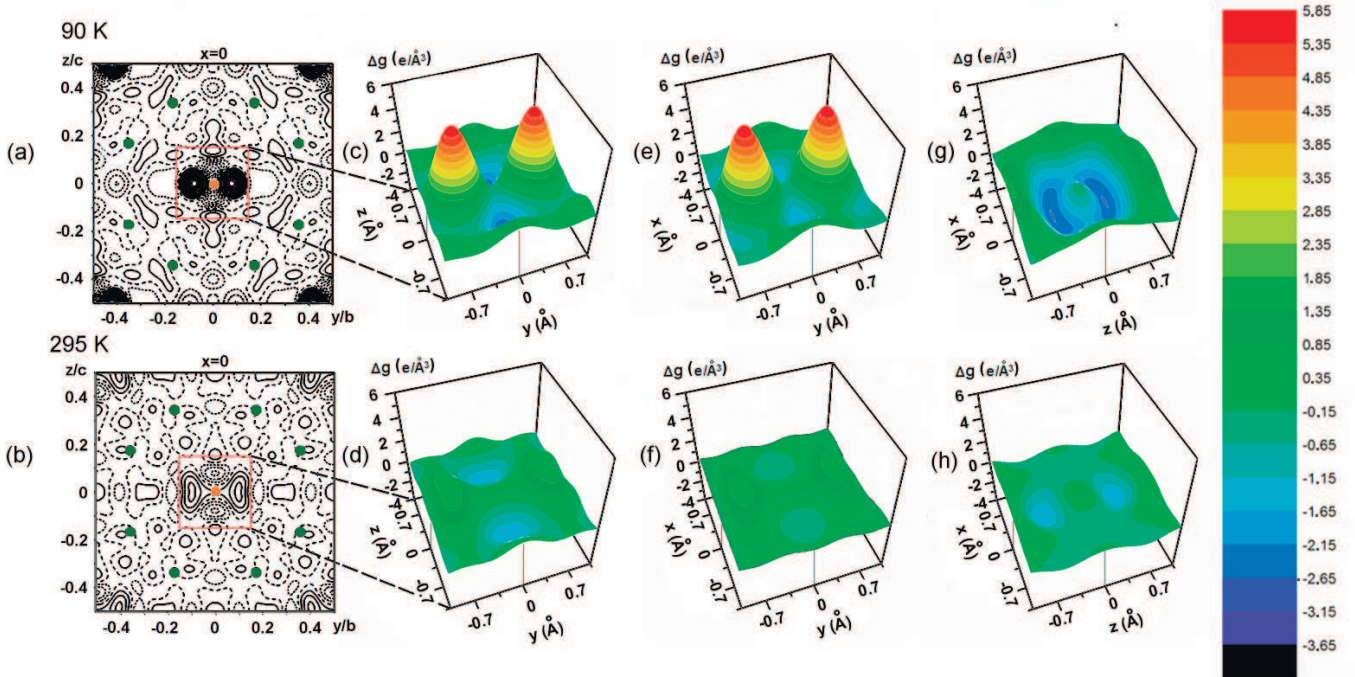


FIG. 3. (Color online) Difference Fourier maps (residual ED $\Delta g, e/\text{\AA}^3$) in the $x = 0$ face of the LuB_{12} unit cell at 90 (a) and 295 K (b), respectively. Red circle is the Lu-site; green circles are B-sites. The (c, d), (e, f) and (g, h) panels are relief drawings of difference Fourier maps made in the vicinity of the Lu-ion, in the $x = 0$, $z = 0$ and $y = 0$ faces of the unit cell, whereas first and second rows of overall picture correspond to temperatures 90 K and 295 K, respectively.

Relief fragments of difference Fourier maps at $x = 0$ (Fig. 3c,d), $z = 0$ (Fig. 3e,f), $y = 0$ (Fig. 3g,h) are presented in three next columns of Fig.3 for better visualization of residual ED distribution near the Lu site. Most notable maxima of residual ED are observed along the y -axis, along which the smaller period $b \neq a \cong c$ is detected (Fig.1). Amplitudes of residual peaks of ED in-

crease significantly with temperature decrease being located $\sim 0.4 - 0.7 \text{\AA}$ away from a central Lu site. Taking temperature behaviour of the unit-cell values into account, the character of structural distortion is closer to tetragonal. Unique y -axis is not an ideal 4-fold axis but can be considered as such a symmetry element to a certain approximation [14].

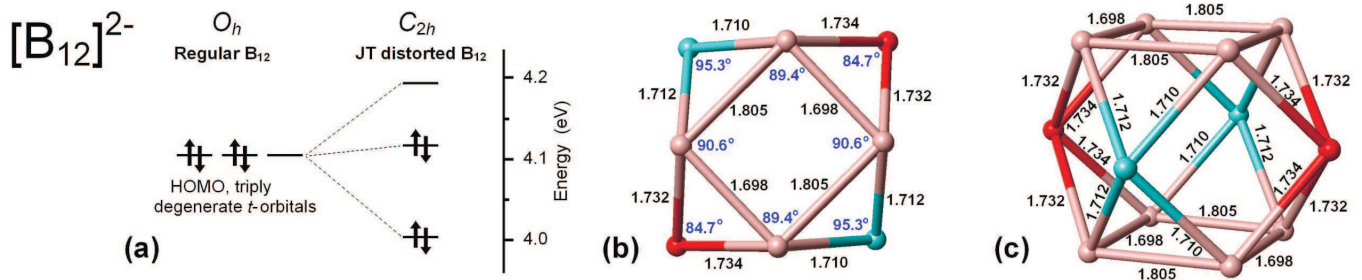


FIG. 4. (Color online) (a) JT splitting of triply degenerate highest occupied molecular orbital with four electrons is indicated. Molecular structure of isolated cluster $[B_{12}]^{2-}$ in the local JT energy minimum as obtained from DFT geometry optimization calculations [14] (projection (b) and perspective view (c)). Principal atomic distances (Å) and bond angles are indicated. The structure exhibits the C_{2h} symmetry. There are three groups of equivalent (symmetry related) boron atoms shown as pink, red, and blue balls.

Discussion. – To understand possible reasons for (i) the symmetry deviation of the LuB_{12} crystal from the cubic one, (ii) the significant anisotropy of the transverse magnetoresistance and the associated non-equivalence of the directions $\mathbf{H}||[00\bar{1}]$ and $\mathbf{H}||[\bar{1}00]$ in the charge carriers scattering (Figure 2d-e, [14]), and (iii) the growth of resistance with the temperature lowering in a steady magnetic field (Fig. 2b), we discuss herein a possible scenario associated with the Jahn-Teller (JT) effect. More specifically, because of triple orbital degeneracy of the ground electronic state, the B_{12} molecules are JT-active and thus their structure is labile due to JT-distortions. In this case, upon decreasing temperature, some intrinsic structural defects (such as boron vacancies and mixed ^{10}B - ^{11}B isotope composition of B_{12} molecules) can lift degeneracy due to symmetry lowering and may cause an electronic phase transition associated with JT structural instability. Similar phase transformations produced by JT-effect of B_{12} icosahedra were earlier observed in higher borides [17].

In order to establish the amplitude and type of the JT distortions in B_{12} cuboctahedra, we performed quantum chemical calculations and geometry optimizations for charged $[B_{12}]^{2-}$ cluster, whose doubly negative charge state is regarded as the most relevant in RB_{12} compounds (see [14]). The structure is shown in Fig. 4. Interestingly, the actual symmetry of the JT distorted cluster (C_{2h}) is lower than the symmetry of tetragonal (D_{4h}) and trigonal (D_{3d}) JT minima expected from the JT theory [18]. The amplitude of the JT distortions of isolated B_{12} clusters is rather pronounced as the bond lengths and bonding angles can vary by $\sim 0.1\text{\AA}$ and $\sim 5^\circ$, respectively (Fig. 4 and [14]).

These results provide evidence that the JT structural liability of B_{12} clusters should play an important role in the microscopic mechanism of lattice distortions of LuB_{12} at low temperatures. Taking into account that B_{12} clusters form an extended 3D covalent network, being connected by B-B covalent bonds, one can suggest that structural JT liability should retain and reinforce in the

boron sublattice of the dodecaborides. The reinforcement due to cooperative dynamic JT effect manifested both in static and dynamic lattice properties may be considered as the cause of large amplitude displacements of Lu atoms in oversized B_{24} cages, resulting in quasi-tetragonal distortions of the *fcc* lattice and the anisotropy of magnetoresistance in LuB_{12} at low temperatures. Therefore, the rattling modes can be attributed to quantum motion of the Lu ions in the double-well potentials (DWPs) with the minima displaced from each other on the distance of $0.4 - 0.7\text{\AA}$ along the *y*-axis (see Figs. 3c and 3e). As a sequence of these large amplitude vibrations of heavy ions the $5d - 2p$ hybridization of electron states along the unique *y*-axis changes dramatically resulting in formation of conductive channels (dynamic stripes [19]) with a strong charge carrier scattering on the filamentary structure. Thus, the proposed scenario may be used to explain naturally the anisotropy of the charge transport in LuB_{12} .

The barrier height $\Delta E = 51 - 97K$ in DWP is detected [20] for LuB_{12} with different numbers of boron vacancies and Zr impurities. Concentration of Lu ions displaced from centres in B_{24} cubooctahedra is estimated to be 3 - 8 at.%. This agrees well with the 3.6 at.% concentration of the off-site Lu ions obtained from the EXAFS measurements at low temperatures [21], where Lu-displacements by $0.2 - 0.3\text{\AA}$ are established.

Conclusion. – Lutetium dodecaboride has been studied here as the model rattling compound to clarify the nature of rattling modes and their influence on the crystal structure and properties. Precision measurements of the crystal structure and charge transport at low temperatures allow detecting the symmetry lowering, which may be attributed to coherent quasi-local vibrations (rattling modes) of Lu ions along singular direction in the dodecaboride lattice. It has also been shown that there is an extra source of lattice instability in LuB_{12} related to the Jahn-Teller effect of B_{12} clusters, which can manifest in concert with displacements of Lu atoms in oversized B_{24} cages resulting in cooperative dynamic Jahn-Teller

lattice distortions and conduction band changes.

This work was partially supported by grants from RFBR No. 15-02-02553, No. 16-02-00171 and by the Ministry of Education and Science of the Russian Federation within the framework of Increase Competitiveness Program of NUST MISiS (project No. 2-2017-023), implemented by governmental decree, N 211. The structure measurements were performed using the equipment of the Shared Research Center FSRC Crystallography and Photonics RAS. One of us (N.S.) acknowledges to V. Moshchalkov and F. Antson for useful discussions.

* nes@lt.gpi.ru

- [1] V. Keppens, D. Mandrus, B. Sales, B. Chakoumakos, P. Dai, R. Coldea, M. Maple, D. Gajewski, E. Freeman, and S. Bennington, *Nature* **395**, 876 (1998); Y. Nakai, K. Ishida, H. Sugawara, D. Kikuchi, and H. Sato, *Phys. Rev. B* **77**, 041101 (2008).
- [2] M. Yoshida, K. Arai, R. Kaido, M. Takigawa, S. Yonezawa, Y. Muraoka, and Z. Hiroi, *Phys. Rev. Lett.* **98**, 197002 (2007).
- [3] G. S. Nolas, J. L. Cohn, G. A. Slack, and S. B. Schujman, *Appl. Phys. Lett.* **73**, 178 (1998); S. Paschen, M. Ikeda, S. Stefanoski, and G. Nolas, in *The Physics and Chemistry of Inorganic Clathrates*, Springer Series in Materials Science, Vol. 199, edited by G. Nolas (Springer Netherlands, 2014) Chap. 9, pp. 249–276.
- [4] K. Asaki, H. Kotegawa, H. Tou, T. Onimaru, K. Matsumoto, Y. Inoue, and T. Takabatake, *J. Phys. Soc. Jpn.* **81**, 023711 (2012).
- [5] Y. Akizuki, I. Yamada, K. Fujita, K. Taga, T. Kawakami, M. Mizumaki, and K. Tanaka, *Angew. Chem. Int. Ed.* **54**, 10870 (2015).
- [6] N. E. Sluchanko, A. V. Bogach, V. V. Glushkov, S. V. Demishev, K. S. Lyubshov, D. N. Sluchanko, A. V. Levchenko, A. B. Dukhnenko, V. B. Filipov, S. Gabani, and K. Flachbart, *JETP Letters* **89**, 256 (2009); P. A. Alekseev, K. S. Nemkovski, J.-M. Mignot, E. S. Clementyev, A. S. Ivanov, S. Rols, R. I. Bewley, V. B. Filipov, and N. Y. Shitsevalova, *Phys. Rev. B* **89**, 115121 (2014).
- [7] P. Alekseev, G. Grechnev, N. Shitsevalova, K. Siemensmeyer, N. Sluchanko, O. Zogal, and K. Flachbart, in *Rare Earths: Research and Applications*, edited by K. Delfrey (Nova, Commack, New York, 2008) Chap. 2, p. 79.
- [8] A. V. Rybina, K. S. Nemkovski, P. A. Alekseev, J.-M. Mignot, E. S. Clementyev, M. Johnson, L. Capogna, A. V. Dukhnenko, A. B. Lyashenko, and V. B. Filipov, *Phys. Rev. B* **82**, 024302 (2010).
- [9] M. Heinecke, K. Winzer, J. Noffke, H. Kranefeld, H. Grieb, K. Flachbart, and Y. B. Paderno, *Z. Phys. B* **98**, 231 (1995); B. Jager, S. Paluch, O. J. Zoga, W. Wolf, P. Herzig, V. B. Filipov, N. Y. Shitsevalova, and Y. B. Paderno, *J. Phys. Condens. Matter* **18**, 2525 (2006).
- [10] J.-M. Mignot, P. A. Alekseev, K. S. Nemkovski, L.-P. Regnault, F. Iga, and T. Takabatake, *Phys. Rev. Lett.* **94**, 247204 (2005).
- [11] H. Weng, J. Zhao, Z. Wang, Z. Fang, and X. Dai, *Phys. Rev. Lett.* **112**, 016403 (2014).
- [12] N. Sluchanko, A. Azarevich, A. Bogach, I. Vlasov, V. Glushkov, S. Demishev, A. Maksimov, I. Tartakovskii, E. Filatov, K. Flachbart, S. Gabani, V. Filippov, N. Shitsevalova, and V. Moshchalkov, *J. Exp. Theor. Phys.* **113**, 468 (2011), [*JETP* **140**, 536 (2011)].
- [13] N. B. Bolotina, I. A. Verin, N. Y. Shitsevalova, V. B. Filippov, and N. E. Sluchanko, *Crystallogr. Rep.* **61**, 181 (2016).
- [14] See “Supplementary materials,” for more information: (Details of experiments, including single crystals growth and characterization (precise x-ray diffraction reflexes [Fig. 1S] and de Haas-van Alphen effect [Fig. 2S]), the schema of magnetoresistance measurements [Fig.S3]. Illustration of a symmetry lowering in LuB₁₂: x-ray data are collected at T = 140 K and difference Fourier maps are obtained when structural symmetry is described using *Fm* $\bar{3}$ *m* (a-c) and *Fmmm* (d-f) groups [Fig. S4]. In depth information on magnetoresistance as obtained for samples #1 and #2 [Figs.S5]. Results of quantum chemical calculations for electrically neutral [B₁₂]⁰ and negatively charged clusters [B₁₂]ⁿ⁻ (n = 1 – 4) with detailed discussion)
- [15] N. Sluchanko, A. Azarevich, A. Bogach, V. Glushkov, S. Demishev, A. V. Kuznetsov, K. S. Lyubshov, V. Filippov, and N. Shitsevalova, *J. Exp. Theor. Phys.* **111**, 279 (2010), [*JETP* **138**, 315 (2010)].
- [16] N. Sluchanko, A. Azarevich, M. Anisimov, A. Bogach, S. Gavrilkin, M. Gilmanov, V. Glushkov, S. Demishev, A. Khoroshilov, A. Dukhnenko, K. Mitsen, N. Shitsevalova, V. Filipov, V. Voronov, and K. Flachbart, *Phys. Rev. B* **93**, 085130 (2016).
- [17] R. Franz and H. Werheit, *EPL (Europhysics Letters)* **9**, 145 (1989).
- [18] I. B. Bersuker and V. Z. Polinger, *Vibronic Interactions in Molecules and Crystals* (Springer, Berlin, 1989).
- [19] D. Reznik, *Physica C: Superconductivity* **481**, 75 (2012).
- [20] N. E. Sluchanko, A. N. Azarevich, S. Gavrilkin, V. V. Glushkov, S. V. Demishev, N. Y. Shitsevalova, and V. B. Filipov, *JETP Letters* **98**, 578 (2014).
- [21] A. P. Menushenkov, A. A. Yaroslavtsev, I. A. Zaluzhnyy, A. V. Kuznetsov, R. V. Chernikov, N. Y. Shitsevalova, and V. B. Filippov, *JETP Letters* **98**, 165 (2013).